



Information Technology and Quantitative Management (ITQM 2014)

A Novel Method in Extracranial Removal of Brain MR Images

Jiahua Du^{a,b}, Gansen Zhao^b, Hao Lan Zhang^a, Jing He^c, Xiaoli Jin^b *

^a SCDM Research Center, NIT, Zhejiang University, 315100, Ningbo, Zhejiang, China

^b South China Normal University, 55 Zhongshan Avenue (West) Tianhe, 510631, Canton, Guangdong, China

^c College of Engineering and Science, Victoria University, Australia

Abstract

The removal of extracranial elements from brain MR images provides doctors a reliable method to analyze and diagnose dynamic data in E-Health. In traditional segmentation, experts are required to identify every element of the whole image, subjectivity and large amount of works make the mission uncertain and intolerant. GVF Snake model leads to efficiently dealing with the segmentation by giving an initial contour around the final object, but manual participation is still inevitable. This paper proposes an automatic morphology-based algorithm to generate the initial contour for active contour model to implement the removal accurately. To achieve the removal, initial contours will be produced by the original contour generator, which are utilized to approach more precise contours implemented by improved GVF Snake model. After a self-correction among the elements, segmentation missions are done. Experimental result shows that with simple steps and little time, the proposed algorithm can complete the segmentation task successfully, and is of good robustness as well as high accuracy.

© 2014 Published by Elsevier B.V. Open access under [CC BY-NC-ND license](https://creativecommons.org/licenses/by-nc-nd/4.0/).

Selection and peer-review under responsibility of the Organizing Committee of ITQM 2014.

Keywords: Medical images processing; Morphology; Initial contour; Contour generator; GVF Snake model

1. Introduction

Image segmentation is widely used in medical image processing, which facilitates the development of E-Health. Removal of extracranial of magnetic resonance (MR) Image as one of its applications, gives doctor a much clearer outline of human brain and decrease the disturbance effectively. Information extract from the processed images can be further used to set up an E-Health data warehouse. However, due to the complex anatomical structure of human brain, it is difficult for even experts to identify every element correctly. Data are nowadays growing rapidly with the speed of which manual segmentation could not catch up with. Manual

* Corresponding author. Tel.: +86-13678931496; fax: +86-020-85211353.

E-mail address: jinxl@sclu.edu.cn.

segmentation exposes some inconvenience and disadvantages [1]. Since recognition vary from person to person result from various medical knowledge background, there is no united roles or standards to define the boundary. The heavy workloads and time costs are also intolerant and impractical, particularly in adapting E-Health and emergency. This obviously brings mistakes into the segmentation.

Active contour model [2] provides a new idea to solve the problem by manually setting a region of interest around certain objects in the MR image. Active contour model, also called Snake, is a parameter-based deformable model defined within an image in the form of curve that can move under the interaction of internal force and external force to approach desired features of an object. However, Snake model has its defect, especially in processing into deep boundary concavities [3]. Although several solutions are proposed to address the problems, like Cohen et al. [4, 5] and Arnaldo et al. [6], most of these solutions solve partial of the problems while creating a new one. It's until Xu and Prince [7] then developed the gradient vector flow (GVF) Snake model that effectively improve the Snake model. After that, series of researches like Wang et al. [8] with NBGVF Snake model, Li et al. [9] with graph theory and Wen et al. [10] with extended balloon and gradient are token to optimize the GVF Snake model.

Hybrid methods are used in brain MR image. Sajjad et al. [11] suggested using morphological operations after detection of false background to improve skull stripping. Liu et al. [12] made an automatically segmentation with adaptive balloon Snake model and pixel clustering. Studies [13, 14] also encourage hybrid approaches to deal with large volume of MR images since each algorithm has its short. This paper combines several methods to propose an automatic algorithm. First, initial contour of MR image will be generated with morphology-based method. With the morphological contour, active contour model implements the removal efficiently. Finally, the segmentation mission is done after a self-correction.

2. GVF Snake Model

Traditional Snake model is defined as a curve $v(s) = [x(s), y(s)]$ $s \in [0, 1]$, from which the energy functional can be represented as follow:

$$E_{snake}^* = \int_0^1 E_{snake}(v(s)) ds = \int_0^1 [E_{int}(v(s)) + E_{ext}(v(s))] ds \quad (1)$$

Where E_{int} and E_{ext} can be realized as the internal and external force. The internal force exists within the curve itself and the external force comes from characteristics of the image. These forces convey energies that causes the movement of the curve until it finally attach to the object. This process can in essence be regarded as minimization energy of a dynamic force formulation.

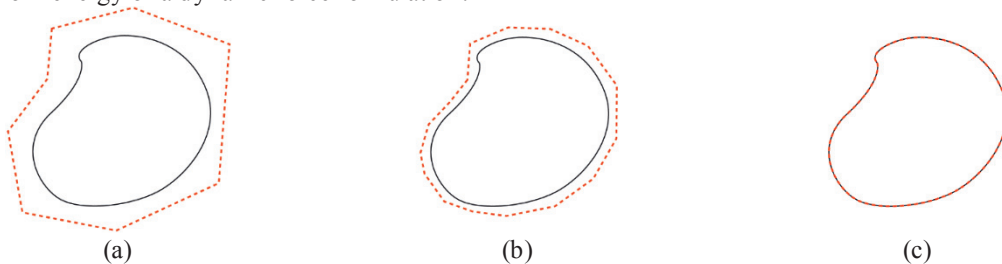


Figure 1: Movement of traditional Snake model. (a) Initial contour is manually selected around the object. (b) Contour that contains energy moves under the influence of internal and external force. (c) The curve is finally converged to the true boundary of the object.

The process that a traditional Snake model minimizes its energy can be viewed as a force balance equation, from which the GVF Snake model replace the external force field with GVF to enlarge the capture range within the image so that the contour can converge to concave boundary effectively. The GVF field is defined as a vector field $V(x, y) = [u(x, y), v(x, y)]$, from which the energy functional can be described as follow:

$$\varepsilon = \iint [\mu\varepsilon_{smooth} + \varepsilon_{gradient}] dx dy \quad (2)$$

Calculating GVF field is in essence a diffusion of the gradient vectors of a gray-level or binary edge map⁷. Once it is computed, the dynamic Snake equation can be solved with similar manner of the traditional Snake model.

3. Improved GVF Snake Model

Statistic data in research [15] shows that, formation of force field and convergence of the curve in GVF Snake model are implemented by iteration. The more iteration it takes, the more resources are required. Orthogonal force field pointing at the true boundary can be found in a small range of space called effective convergence area surrounding the true boundary. Since the curve is influenced by external force, if initial contour is close enough to the described area, the curve still converge correctly even iteration is reduced.

This paper proposed a morphology-based algorithm that produces initial contour near effective convergence area. To achieve the goal, we preform two layers that dynamically generate the curve shape of the corresponding MR image. Those curve shapes will be combined and transformed in a specific manner, and the initial contour is produced. After the segmentation of all MR images, results need to be checked and adjusted using self-adaptive model in order to make a better performance.

3.1. Contour Generator

3.1.1. Island layer

In this layer, we use “Island” pattern to produce curve shape of current MR image. To achieve this generation, Image first need to be converted into a binary form by filtering Otsu threshold selection [16]. We regard this binary image as a map, from which the background is ocean and the foregrounds are collections of islands. We define one of the islands and its surrounding as center and effective area. Each island is connected to the centric element with rope, islands are changing from active to inactive as distance grows. The center intends to find a stable state by attracting all other islands and discarding those are too inactive. Theoretically, this is a process of minimizing the dispersion degree of centric element and the others.

Given a binary image $I(x, y)$ and its boundary B that its foreground collection F contains $n(n \in N^*)$ elements, define C as centroid, the operations can be described as follow:

- (1) Set $C_B(x, y)$ as default centroid, calculate distances $d(j)$ between $F(j)(j \in N^*, j \leq n)$ and $C_j(x, y)$.

$$d(j) = \sqrt{[C_j(x) - C_B(x)]^2 + [C_j(y) - C_B(y)]^2} \quad (3)$$

- (2) Denote C_p as the minimum value of $d(j)$ and default centroid, again calculate distances $D(j)$ using (3) and mark D_{max} and D_{min} as the maximum and minimum value. Normalize $D(j)$ using linear function.

$$N(j) = \frac{D_j - D_{min}}{D_{max} - D_{min}} \quad (4)$$

(3) Calculate the standard deviation of $N(j)$.

$$STD = \frac{1}{n} \sum_{j=1}^n \left(N(j) - \frac{1}{n-1} \sum_{j=1}^n N(j) \right)^2 \tag{5}$$

(4) Given a threshold T_v , we consider the centric element is stable. When $STD \leq T_v$. If $STD > T_v$, it implies that the dispersion degree of islands are large, removing any of the elements may reduce STD .

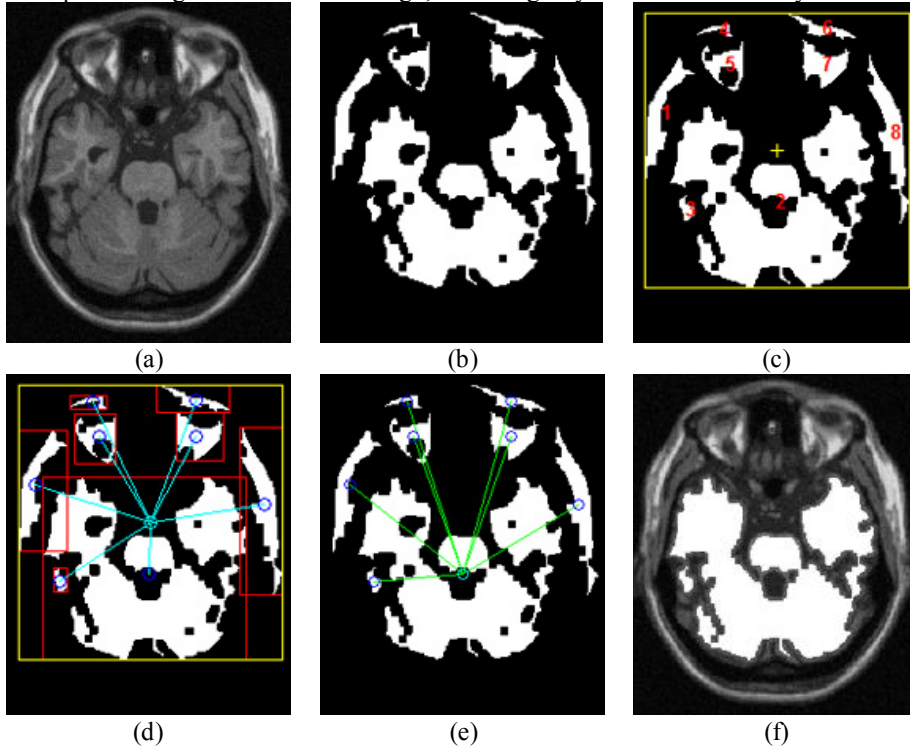


Figure 2: Demonstration of island layer. (a) Original MR image. (b) Image is processed with Otsu threshold selection. (c) The boundary and initial centroid of (b) is calculated, islands in the image are marked numerically. (d) Choosing a new centroid determined by the distance. (e) Gathering or discarding other islands to form a stable state. (f) Final result.

3.1.2. Ellipse layer

In this layer, we use “Ellipse” pattern to produce curve shape of current MR image. To achieve this generation, we construct a discrete sphere model based on human brain structure, from which each slice could be obtained. When extracting a slice from the sphere model, the slice are calculated and relocation by aligning the centroid of the MR image.

Given the quantity of MR images H , a binary image $I(n)$ and its boundary B and, define C as centroid, $a(n)$ as semi-major axis and $b(n)$ as semi-minor axis, the curve shape can be described as follow:

$$f = \frac{b(n)}{(x_n - C_n(x))^2} + \frac{a(n)}{(y_n - C_n(y))^2} - 1 \tag{6}$$

$$a(n) = b(n) = ORI + \sin t \left(\frac{B}{2} - ORI - PAD \right) \quad (7)$$

Where ORI and PAD are offset factors to limit the growth of semi-major and semi-minor axis, $t = n\pi/2H$ is a dynamic coefficient that controls the scale of the curve shape and it is determined by the quantity of MR images H and position of slices n .

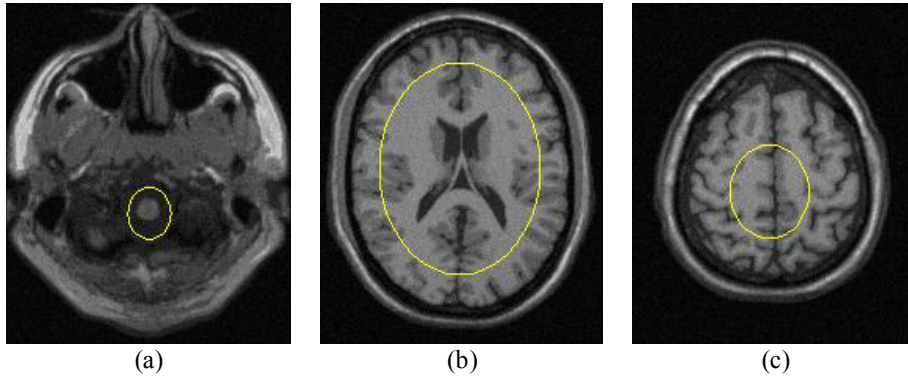


Figure 3: Demonstration of ellipse layer.

3.1.3. Overlapping, outlining and ordering

Both the island layer and the ellipse layer have their advantages, the former one is close to the true boundary in the outermost edge, while the latter one is of high connectivity in the center position. Since traditional GVF Snake model have only one snake, that is to say it can deal with only one object simultaneously. As a complement, we combine the island layer and ellipse layer together by overlapping to form a new curve shape. We introduce canny edge detector to extract the outline of the hybrid layer. To implement GVF Snake model, the parametric inputs for active contour have, in general, the following requirement:

- (1) Parameter inputs are discrete. Though the definition of the active curve is continuous, we need to launch the model with discrete data in computer science. In this case, the shape curve can be divided into points by sampling in a certain rate and optimized with other technologies.
- (2) Parameter inputs comply with some specific order. Loading points into parameter with a horizontal or vertical direction will cause an exception, let alone a random way. The accepted methods to load points into parameter are clockwise or anticlockwise. In this case, points to be loaded can be classified, filtered and re-ordered based on their original coordinates at the axis.

Given a pixel collection P result from the edge of the curve shape contains $n(n \in N^*)$ points, the height and width of its boundary $B(h)$ and $B(w)$, define C as centroid, the pixel collection can be classified as follow:

$$\begin{cases} P'(n) \in L_1, & x_n \in \left[r - \frac{B(w)}{2}, r \right) \\ P'(n) \in R_1, & x_n \in \left(r, r + \frac{B(w)}{2} \right] \\ P'(n) = \emptyset, & x_n \in A(x, y) \end{cases} \quad (8)$$

Where the r is an offset factor to limit the scan area of the classifier, $A(x, y)$ implies discarding area, which can be defined due to different situations. We now separate the pixel collection into two containers as L and R , in order to simplified members, greedy algorithm are introduced to eliminate redundant points efficiently. Define MIR as a mirror function that create a new point reflected along a vertical axis, the pixel collection can be filtered as follow:

$$\begin{cases} L_2(k) = u_{min}, & u \neq \emptyset \\ L_2(k) = MIR(R_2(k)), & u = \emptyset \\ R_2(k) = v_{max}, & v \neq \emptyset \\ R_2(k) = MIR(L_2(k)), & v = \emptyset \end{cases} \quad (9)$$

Define FLI as a flip function that create a new point reflected along a horizontal axis, the pixel collection can be ordered as follow:

$$\begin{cases} C^{(1)} = L_2(k) \cup FLI(R_2(k)) \\ C^{(2)} = FLI(L_2(k)) \cup R_2(k) \end{cases} \quad (10)$$

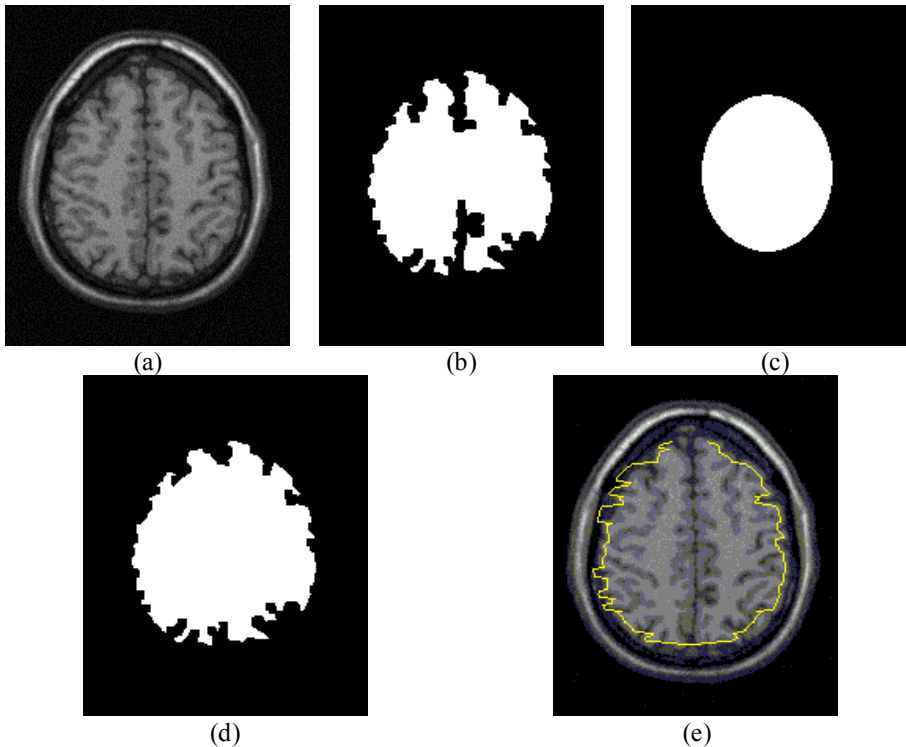


Figure 4: Demonstration of overlapping, outlining and ordering. (a) Original MR image. (b) Curve shape generated by island layer. (c) Curve shape generated by ellipse layer. (d) Overlapping. (e) Outlining and ordering.

3.2. Self-Reviser

Since brain MR images are discrete sequences obtained from the continuous signal from MRI, much of the similarities exist among images. With this observation, we can simulate a new brain MR images by exploiting bilateral images with series of calculating. Hence, it's a reliable way to detect and correct mistakes caused by the GVF Snake model or layers. Thus, the broken images can be fixed hopefully.

In this paper, we proposed an n -size slide window to detect exceptions from the whole sequences of brain MR images. This slide window is designed to move on the histogram of accuracy rate of the segmentation results, it can detect concave point or platform and attempt to implement revision so that they owe a better segmentation quality. The size implies the length of the slide window moving from the beginning to the end in image sequences. If n equals to 3 and exception is found, slide window will attempt to revise the broken image with similarities of images located at the first and last position of the window. If n equals to 5 under the same situation, images located at the second and penultimate place will be revised by the first and last position, which leaves the question as a 3-size slide window problem. Cases on different n in the slide window have the same solution.

This paper, generally, use slide windows with size equals to 3, 4 and 5 simultaneously. Due to the mechanism of slide window, there will be a relatively monotone increasing and decreasing section at the beginning and the end of the histogram, we use another slide window with the same idea to improve the segmentation quality.

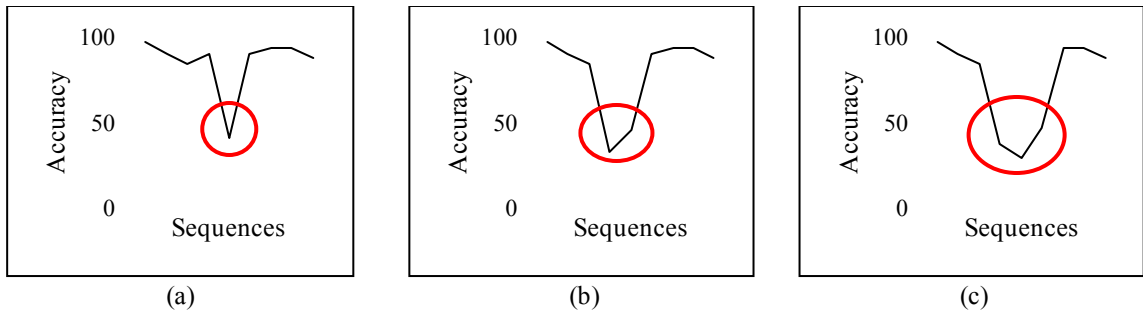


Figure 5: Mechanism of n -size slide window. (a) 3-size slide window. (b) 4-size slide window. (c) 5-size slide window.

4. Implementation and experiment results

4.1. MR image data

This paper exploits simulated brain database (SBD) [17] from McConnell Brain Imaging Centre (BIC) as materials to evaluate the proposed algorithm. SBD contains a set of realistic MRI data volumes and respective ground truths, which can be orthogonally view in a transversal, sagittal, and coronal aspect. The anatomical structure of human brain in BIC is consist of 10, including background, cerebrospinal fluid (CSF), grey matter (GM), white matter (WM), fat, muscle-skin, skin, skull, glial matter, connective. Extracranial removal is defined as the process of preserving only CSF, GM, WM and glial matter.

More than 10 parameters are required to configure before SBD can simulate the desired example, we here discuss the noise level and the intensity non-uniformity (INU) level that related to this paper, while others are set as default. There 6 level of noise, 0%, 1%, 3%, 5%, 7% and 9%, while 3 level of INU, 0%, 20% and 40%. Each example contains 181 slices in, we define effective area are slices from 10 to 154 since the corresponding ground truth is empty out of this range. Generally, we use example with 5% noise level and 20% INU level as default material.

4.2. Measurement and environment

In this paper, we use Jaccard Similarity (JS) [18] and standard deviation to evaluate the accuracy and robustness of the proposed algorithm. All experiments are programmed with MATLAB R2010b (64-bit) and implemented under Windows 8.1 (64-bit) with Intel Core 2 DUO P8700 (2.53 GHz) and 2G memory.

4.3. Accuracy

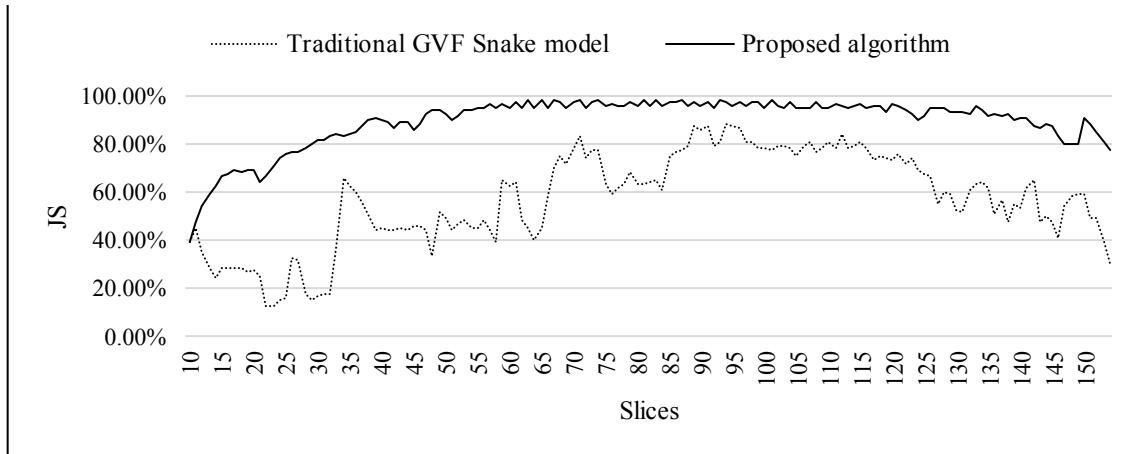


Figure 6: Accuracy of segmentation results

To evaluate the accuracy, we separately launch traditional and improved Snake model with default sample. Since traditional GVF model consist of no initial contour, we use ellipse layer to generate it instead. From the data, we know that the proposed algorithm finish the task with accuracy of 89.01%, almost 1.6 times better than the traditional algorithm in segmentation quality while it only gets 56.72% as result. Moreover, performance of the proposed algorithm is more stable with standard deviation equals to 0.1077, which is nearly half of the traditional model with 0.1963.

4.4. Robustness



Figure 7: Robustness analysis

To evaluate the robustness, we put forward 6 experiments with different samples to form a comparison. Since robustness should be checked in a more disturbed environment, there is no need to examine samples carry lower noise or INU level than default. Thus, the test materials include samples with 7% noise and 20% INU level, 9% noise and 20% INU level, 7% noise and 40% INU level, 9% noise and 40% INU level as well as the default sample using both the traditional and improved approach.

We calculate the standard deviation of accuracy of each slice by combining all results. From the data, we know that the proposed algorithm is stable and has a strong robustness to deal with various disturbances comes from noise or INU with the highest standard deviation 0.2403, which is lower than 0.25.

4.5. Time cost

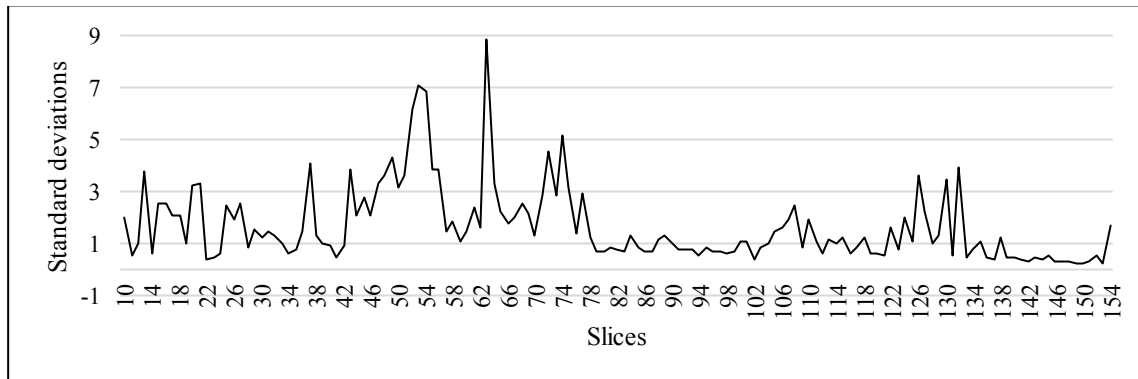


Figure 8: Time cost analysis

To evaluate the time cost, we suggest the same experiments as evaluation of robustness to form a comparison. Since the improved GVF Snake model introduce new concept of self-reviser, consuming time cost is added after the first segmentation. However, the extra time devoted to smoothen the wave-liked curves of histogram has an effect on the whole sequences of MR images. We can thus eliminate the extra time by distributing it to all slices equally.

We calculate the standard deviation of time cost of each slice by combining all results. From the data, we know that the proposed algorithm have a relatively unstable performance in time cost. The unstable situation result from the uncertain time cost for GVF Snake model to converge to the true boundary. All in all, the average time cost still has a nearly 10% reduced from 3.630 to 3.3108, which is satisfied.

5. Conclusion

This paper proposes a morphological algorithm to implement the following removal mission automatically by generating the initial contour for active contour model. Promising results demonstrate that the proposed algorithm shows good performance and can complete the segmentation task successfully with simple steps and little time, and is of strong robustness as well as high accuracy rate.

References

- [1] Das B., Banerjee S. Parametric contour model in medical image segmentation. In: Suri JS., Farag AA, editors, *Deformable models, topics in biomedical engineering*. International Book Series, Springer New York; 2007, p. 31–74.
- [2] Kass M., Witkin A., Terzopoulos D. Snakes: Active contour models. *Int. J. Computer Vision*, 1987; 1(4):321-331,.

- [3] Davatzikos C., Prince J. L. An active contour model for mapping the cortex. *IEEE Trans. on Medical Imaging*, 1995; 14(1):65-80.
- [4] Cohen L., Cohen L., Finite-element methods for active contour models and balloons for 2-d and 3-d images. *Pattern Anal Mach Intell IEEE Trans*, 1993; 15(11):1131–1147.
- [5] Yu L., Fan Y., Liu C. Research of Time about GVF Snake Model, *Computer Engineering and application*, 2006; 35:33-36.
- [6] Abrantes AJ, Marques JS. A class of constrained clustering algorithms for object boundary extraction, *IEEE Transactions on Image Processing*, 1996; 5(11):1507–1521.
- [7] Xu CY, Prince J. 1997 “Gradient vector flow: a new external force for snakes,” 1997 IEEE Computer Society Conference on Computer Vision and Pattern Recognition, p. 66–71.
- [8] Wang YQ, Liu LX, Zhang H, Cao ZL, Lu SP, Image segmentation using active contours with normally biased GVF external force. *Signal Process Lett IEEE*, 2010; 17(10):875–878.
- [9] Li CM, Liu JD, Fox M. 2005 “Segmentation of edge preserving gradient vector flow: an approach toward automatically initializing and splitting of snakes,” 2005 IEEE computer society conference on Computer vision and pattern recognition. vol 1. p. 162–167.
- [10] Huang WB, Yan Y., Wang YJ. Boundary Segmentation Based on Improved GVF Snake Model. *Advanced Materials Research*, p. 3920-3923.
- [11] Mohsin S, Sajjad S., Malik Z., Abdullah AH, Efficient way of skull stripping in MRI to detect brain tumor by applying morphological operations after detection of false background, *International Journal of Information and Education Technology*, 2010; 2(4).
- [12] Liu HT, Sheu T WH, Chang HH. Automatic segmentation of brain MR images using an adaptive balloon snake model with fuzzy classification, *Med Biol Eng Comput*, 2013; 51:1091–1104.
- [13] Boesen K, Rehm K, Schaper K, Stoltzner S, Woods R, Lders E, Rottenberg D. Quantitative comparison of four brain extraction algorithms. *NeuroImage*, 2004; 22(3):1255–1261.
- [14] Fennema-Notestine C, Ozyurt IB, Clark CP, Morris S, Bischoff- Grethe A, Bondi MW, Jernigan TL, Fischl B, Segonne F, Shattuck DW, Leahy RM, Rex DE, Toga AW, Zou KH, Brown GG. Quantitative evaluation of automated skull-stripping methods applied to contemporary and legacy images: effects of diagnosis, bias correction, and slice location. *Hum Brain Mapp*, 2006; 27(2):99–113
- [15] Cohen LD, On active contour models and balloons, 14th International Conference on Graphical Models and Image Processing, 1991;53:211–218.
- [16] Otsu N. A Threshold Selection Method from Gray-level Histogram. *IEEE Trans on Systems, Man and Cybernetics*, 1979; 9(1): 62-66.
- [17] Cocosco CA, Kollokian V, Kwan RKS, Evans AC, 1997. “BrainWeb: Online Interface to a 3D MRI Simulated Brain Databas NeuroImage.” 3rd International Conference on Functional Mapping of the Human Brain, vol.5, no.4, Copenhagen.
- [18] Vovk U, Pemus F, Likar B. A review of methods for correction of intensity inhomogeneity in MRI. *IEEE Trans Med Image*, 2007; 26:405–21.